Land Cover Classification by using Sentinel-2 Images: A case study in the city of Rome

M. Majidi Nezhad[1], A. Heydari[1], L. Fusilli[2], G. Laneve[2]
[1]Department of Astronautics, Electrical and Energy Engineering (DIAEE), Sapienza University of Rome
Rome, Italy
meysam.majidinezhad@uniroma1.it; azim.haydari@uniroma1.it
[2]School of Aerospace Engineering, Sapienza University of Rome
Rome, Italy
lorenzo.fusilli@uniroma1.it; giovanni.laneve@uniroma1.it

Abstract - Land cover mapping of land area in Mediterranean climate regions from satellite images is not simple, due to the similarity of the spectral characteristics of the urban area and city surroundings. In this study, satellite images from Sentinel 2A by ESA (European Space Agency) were used to classify the land cover of Rome city, Italy. This paper presents two methods aiming at improving the land cover classification accuracy by using multispectral satellite images. The classification process was performed by using two different algorithms, namely: Maximum Likelihood (ML) and Support Vector Machine (SVM).
The supervised "Maximum Likelihood" and "Support Vector Machine" classification algorithms available in ENVI (Environment for Visualizing Images) software, were used to detect five land cover classes: urban, forest, water, agriculture and empty land classes. The results show the ML method applied to Sentinel-2A images provides a higher overall accuracy and kappa coefficient than the SVM method. The main reasons are to increase two amounts in the ML method and over the next few years in this study, first: carry out three steps for increase accuracy and kappa with Sieve Classes, Clump Classes and Majority/Minority Analysis. And second reason the most accurate classification for both approaches was allocated to the year 2018, possibly due to the higher image quality and on-time training sample sites compared to previous 2015, 2016, 2017 years. The results of both methods in this study have been compared.

Keywords: Land cover mapping, Sentinel 2A, Supervised Classification, Maximum Likelihood (ML), Support Vector Machine (SVM), Confusion Matrix.

1. Introduction

In last centuries, the trend in the urban population growth is accompanied by an increase in the land area merged in cities and around the cities [1], causing several issues linked to the dense concentration of inhabitants causing social and environmental issues such as concentrated pollution. In the present paper, the changes in the environment due to the strong population increase has been studied by means of land cover mapping classification through the Sentinel-2 images. Land cover mapping classification of the different land areas could provide vital information in several fields, such as: environmental science [2-3], risk assessment [4-6], urban management [7-8], regional planning [9-11], sustainable development [12-15], urban growth assessment [16]. Therefore, updated land cover mapping could play an essential role in maintaining the harmony between the city and the hinterland. The Copernicus programme formerly (GMES), Global Monitoring for Environment and Security, is an operational programme of earth observation, which made the access to satellite based information timely and easily in many application domains such as: land [17][19], marine [20-22], atmosphere [23-24], emergency response [25], climate change [26], Security and Safety [27].

Sentinel-2 was launched by ESA (European Space Agency) for global monitoring. The Sentinel-2 Multispectral Imager (MSI) sensors have very different spatial and temporal resolutions (10 to 60m) [28]. Many studies on land covering analysis and mapping have been conducted in large area with different satellites images such as: Landsat 8 [29] and SPOT 4 [30], SPOT 5 [31], Worldview II and III [32], ENVIsat and ASAR [33], Landsat MMS [34] and also many methods of accuracy assessment have been discussed in the remote sensing literature by Aronoff, 1982 [35], Kalkhanl, 1995 [36], Koukoulas & Blackburn, 2001 [37], Rosenfield & FitzpatrickLins, 1986 [38]. The most widely promoted and used, may be derived from a confusion matrix (CM) [39]. Lefebvre et al [40], by using Landsat and Sentinel 2 satellites images described a methodology based on an approach which relies on independent image classifications that are fused using the Dempster–Shafer theory.
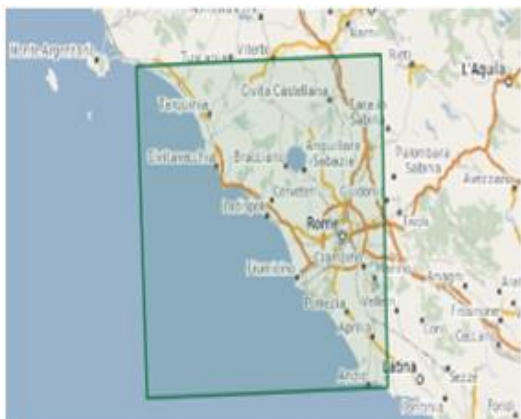
Methodology presented in this study can be used in any other land cover classification task using regular acquisitions issued, for example, from Sentinel 2 satellite. Zakeri et al [41], explained by using ALOS-2 PALSAR-2, Sentinel-1 satellites images for land cover classification of Tehran city and used two supervised classification algorithms, Support Vector Machine (SVM) and Maximum Likelihood (ML), to detect land, vegetation, and three different built-up classes. The results by Zakeri et al showed the layer stacking of texture features and backscatter values significantly increases the overall accuracy.

Rome city is the largest municipality in Europe and the largest rural municipality in Italy country. The spatial distribution of buildings within the municipality is distinctive. Unbuilt areas comprise 73 percent of the territory [42]. This paper is structured as follows: Section 2 describes the study area and the data; Section 3 presents the proposed methodology; Section 4 is dedicated to the results; Section 5 highlights the main findings and the implications of this study. All processes in this study were carried out by using ENVI 4.8 (Environment for Visualizing Images) software.

2. Study Case

The present study aims at carrying out a land cover classification with satellite images from Sentinel 2A. To reach this goal one climate region case study area with different crops (Table 1) and population was selected. The city of Rome (Fig 1), Italy, which is one of the most populated and urbanized areas in Italian country, was selected. The city covers near 5352 km^2. The territory mainly consists of hills (50%), lowlands (30%), and mountains (20%). Rome, such as other Mediterranean cities, went through a rapid transition from the historic compact model to a scattered and polycentric urban form, characterized by huge expansion around the urban area [43].

Table 1. (Right) Characteristics of the test area: location, extent, climate and soils.

Area	Rome
Zone	UTM-33N
World Geodetic System (WGS)	WGS-84
Latitude/ Longitude	41.890251 12.492373
Extent (Pixel)	1418 x 1216
Climate	Mediterranean
Average annual temperature (°C) 2017	16
Average Precipitation (mm) 2017	69.77

Fig. 1: (Left) Location of Rome city and footprint of the Sentinel 2A images tale used in this study (green square).

The images used in this paper were acquired by Sentinel 2A satellites, operated by ESA, this satellite was launched in 23 June 2015. Time images case studies (2015.12.18-2016.07.08- 2017.04.21-2018.04.26) with all spatial and spectral characteristics correspond to a Sentinel - 2A Level 1C product S2A_MSIL1C and OPER_MSI_L1C_TL_SGS. The images were downloaded by Copernicus web site (https://scihub.copernicus.eu/) with the total bands (Table 2). The images provided by the Sentinel satellite family are available for free and open source toolboxes were employed for pre-processing them. The images were projected on the WGS84 reference (Semi- Major Axis: 6378137 m and Flattening: 298.257223563) ellipsoid and zone Rome, UTM zone 33. The first step consists of Geo-referencing all bands and then make a layer stacking by using the ENVI software. As the last step, the Sentinel 2A images were cut by using a ROI (region of interest) tool for better focusing on the case study area (Fig 2). In this study we use a pseudo-natural colour RGB composite images and then an Enhance liner (0-225) for show the images (Fig 2) and subset data via ROIs tool for next step.

Table 2: (Right) The bands of the MSI sensor on board of Sentinel-2 used in this study, their central wavelengths and spatial resolutions.

Bands	Central wavelength (μm)	Resolution (m)
Band 2 – Blue	0.490	10
Band 3 – Green	0.560	10
Band 4 – Red	0.665	10
Band 5 – Vegetation Red Edge	0.705	20
Band 6 – Vegetation Red Edge	0.740	20
Band 7 – Vegetation Red Edge	0.783	20
Band 8 – NIR	0.842	10
Band 8a – Vegetation Red Edge	0.865	20
Band 11 – SWIR	1.610	20
Band 12 – SWIR	2.190	20

Fig. 2: (Left) Rome city, RGB (R:4 G:8 B:3) image with enhancement (Liner 0-225).

3. Methods

ROI tool was used for defining some samples areas to train the classifier algorithms such as: urban, forest, water, agriculture and empty land. The classification process was performed using two different algorithms: ML and SVM. These two classification algorithms are derived from statistical theories and commonly used in land cover classification studies [44]. The processing procedure for supervised classification based on ML and SVM are schematically shown in Fig 3 and Fig 4.
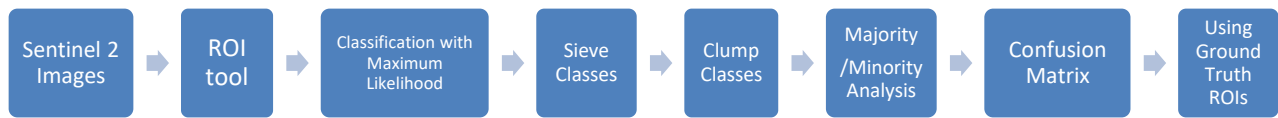

Fig. 3: Flowchart methodology of land cover mapping classification using the Sentinel 2A images with Maximum Likelihood (ML) in ENVI software.

Fig. 4: Flowchart methodology of land cover mapping classification using the Sentinel 2A images with Support Vector Machine (SVM) in ENVI software.

Training samples must be selected based on a homogenous group of image pixels to give the best reparability. Therefore, monitoring the study area and assessing the several land covers is necessary before selecting the training samples. Additionally, applying the appropriate algorithm to identify the homogeneity of the training data to group the pixel values of a dataset is important. At the end, of the classification process, the accuracy of the results from the ML and SVM methods was measured by calculating a CM. The CM is a standard method used to evaluate the classification accuracy in remote sensing satellites images [45].

The pixel oriented supervised classification of Sentinel 2A Satellite images represents a problem of estimating the probability density. Based on training data for each class, the probabilities are estimated for all classes and then used to classify all the pixels in the image. The ML method works on the assumption that each class is normally distributed. In this method, for each pixel, the probability that it belongs to a specific class is calculated. Then, the pixel is assigned to the class that yields the highest probability [1]. The SVM was developed in recent years, increased for land cover classification often

used in remote sensing [46]. The SVM separates the pixels of an image using optimal hyper planes that maximize the margin between the classes. The data points closest to a hyper plane are called support vectors. A nonlinear classification can be performed using kernel functions to the support vectors [47-48].

In the classification, there are two possible errors that can be committed in assigning a pixel to a certain class, an omission error occurs when the pixel is assigned to the wrong class, whereas a commission error occurs when a pixel from another class is assigned to the class under consideration. To assess the extent of this error and therefore the quality of the classification, the CM is introduced. The omission errors are represented by the out of diagonal values along the column instead and the commission errors are represented by the out of diagonal values in the row direction (Table 4). The elements along the diagonal represented the pixels assigned correctly. The omission error, for each class, whose complement is called producer accuracy is calculated as the ratio between the pixels of the main diagonal and the total pixels recognized as belonging to that particular class. As for the commission error and its complement said user accuracy, the calculation is made considering the ratio between the pixels on the diagonal and the sum of row elements corresponding to a certain class. In this study, not only the overall accuracy and kappa coefficient showed in CM, but also commission and omission, producer and user accuracies per pixel for each classes are calculated from CM. The CM was prepared using truth data over the five land cover classes, based on the comparison of the CM of the classification results.

4. Results

This paper aims to obtain a land cover mapping of the Rome city with the best accuracy by using Sentinel 2A images. The performance of the supervised classification algorithms, ML and SVM were assessed. The images by using all channels shown in Table 2 classified and analysed with different tools in ENVI software. To validate the classification result, we computed the CM using the ground truth data. Fig 5 shows the classification results by for the ML and SVM techniques in this software for 2018. In this classification using ROI Tool for classification images in five classes (Urban, Forest, Water, Agriculture and Empty Land).
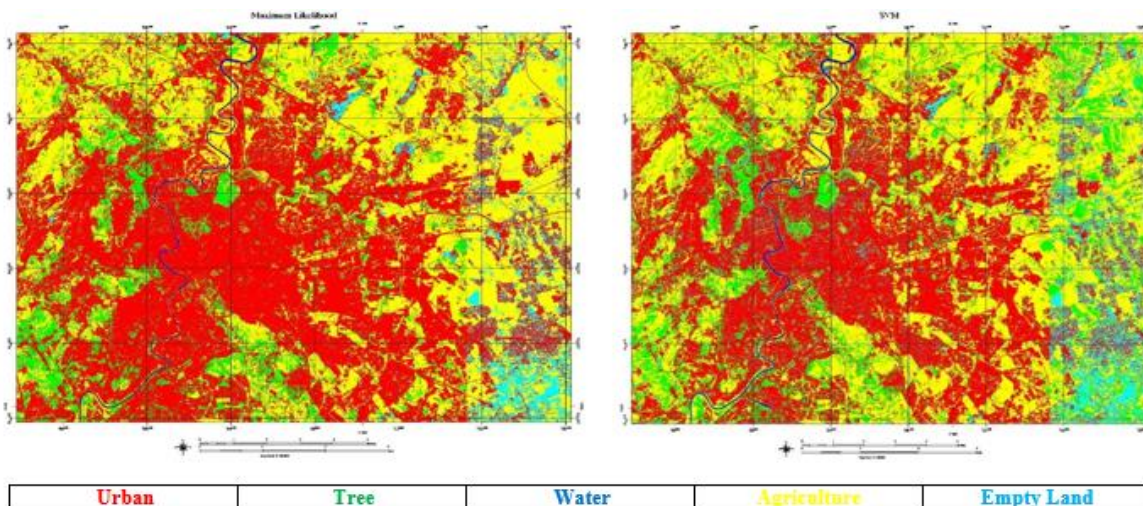

| Urban | Tree | Water | Agriculture | Empty Land |

Fig. 5: Maximum Likelihood (left) and Support Vector Machine (right) results for Rome in 2018.

4.1. Maximum Likelihood (ML)

The CM results for the ML technique show highest overall accuracy and kappa coefficient for all the four acquisition date. Table 3 shows these values according the five different classes for four years. The CM includes the Commission (producer accuracy) and Omission errors (user accuracy) as well (Table 4). The diagonal elements in these tables depict the correctly classified pixels in each land cover classes. To increase the accuracy in the supervised classification from Sentinel 2A images, a post-classification processing, including Sieve classes, Clump classes and majority/minority analysis, was applied for each image, these tool significantly increases the overall accuracy.

4.2. Support Vector Machine (SVM)

The CM results achieved by SVM technic always shows overall accuracy and kappa coefficient values lower than ML method. Table 3 shows these parameters by the CM with Ground Truth from SVM. Table 4 shows five classes according the pixels, the commission, and omission error and commission error for the CM results.

Table 3: Results table with ML and SVM classification method.

Year	2015		2016		2017		2018	
Classification	ML	SVM	ML	SVM	ML	SVM	ML	SVM
Accuracy	95.02%	83.94%	95.20%	82.15%	86.71%	83.22%	100.00%	93.17%
Kappa	0.92	0.76	0.93	0.73	0.81	0.75	1.00	0.90

Table 4: Confusion matrix results with ML and SVM classification methods for Two years.

ML Confusion matrix 2018

Class	Urban	Forest	Water	Agriculture	Empty Land	Commission	Omission	Prod. Acc.	User Acc.
Urban	1196	0	0	0	0	0/1196	0/1196	1196/1196	1196/1196
Forest	0	394	0	0	0	0/394	0/394	394/394	394/394
Water	0	0	20	0	0	0/20	0/20	20/20	20/20
Agriculture	0	0	0	1323	0	0/1323	0/1323	1323/1323	1323/1323
Empty Land	0	0	0	0	424	0/424	0/424	424/424	424/424
Total	1196	394	20	1323	424				

SVM Confusion matrix 2018

Class	Urban	Forest	Water	Agriculture	Empty Land	Commission	Omission	Prod. Acc.	User Acc.
Urban	1119	0	0	0	106	108/1227	77/1196	1196/1196	1119/1227
Forest	5	373	0	2	1	28/401	2/394	373/394	373/401
Water	0	0	20	22	0	0/20	0/20	20/20	20/20
Agriculture	8	19	0	1299	0	27/1326	24/1323	1299/1323	1299/1326
Empty Land	64	2	0	0	317	66/4383	107/424	317/424	317/383
Total	1196	394	20	1323	424				

ML Confusion matrix 2017

Class	Urban	Forest	Water	Agriculture	Empty Land	Commission	Omission	Prod. Acc.	User Acc.
Urban	1196	0	0	0	10	18/1214	0/1196	1196/1196	1196/1196
Forest	0	370	0	0	91	106/476	24/394	370/394	370/476
Water	0	0	20	0	0	0/20	0/20	20/20	20/20
Agriculture	0	0	0	1026	22	28/1054	297/1323	1026/1323	1026/1054
Empty Land	0	18	0	0	299	292/591	125/424	299/424	299/591
Total	1196	394	20	1323	424				

SVM Confusion matrix 2017

Class	Urban	Forest	Water	Agriculture	Empty Land	Commission	Omission	Prod. Acc.	User Acc.
Urban	1141	0	1	28	4	33/1174	55/1196	1141/1196	1141/1174
Forest	1	257	0	65	139	205/462	137/394	257/394	257/462
Water	2	0	18	22	0	2/20	2/20	18/20	18/20
Agriculture	51	34	1	1197	100	186/1323	126/1323	1197/1323	1197/1383
Empty Land	1	103	0	0	181	137/318	243/424	181/424	181/318
Total	1196	394	20	1323	424				

According to the confusion matrix, the overall accuracy of the ML classification was better than SVM classification. This was also the case for the overall kappa statistics. Overall accuracy ranged between 86.71% and 100% for ML approach and 82.15% and 93.17% for the SVM. In first way (ML method) of this study: after finish classification with ML carry out three steps for increase accuracy and kappa. Step1, by using sieve classes to solve the problem of isolated pixels occurring in classification satellite images (Fig 6 A). Step 2, in this step by use clump classes to clump adjacent similarly classified

areas together using morphological operators (Fig 6 B). Step 3, at the end step, by use Majority/Minority Analysis to classification satellite (Sentinel 2) images (Fig 6 C). The most accurate classification for both approaches was allocated the year 2018, possibly due to the higher image quality and on-time training sample sites.
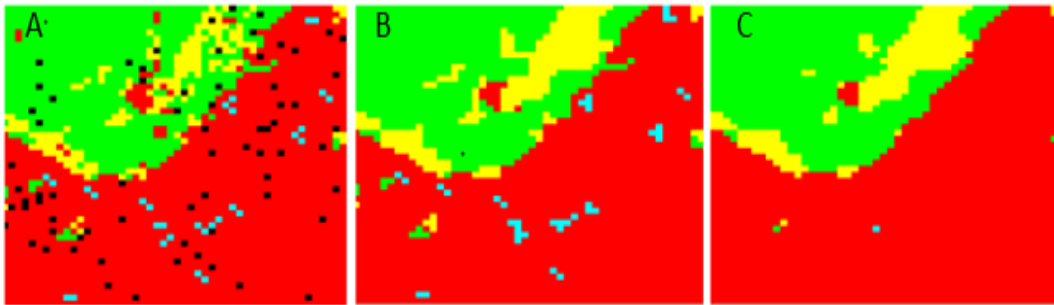

Fig 6. A) Sieve classes, B) Clump classes, C) Majority/minority analysis.

5. Conclusion

In this paper, to improve the supervised classification method with ML and SVM algorithm by images from Sentinel 2A for land cover mapping in ENVI software. For this target, Rome city were selected as the study areas. The CM results by using ground truth ROIs were found to be high overall accuracy for Rome city. The overall accuracy and the kappa coefficient were used to compare the two methods. By this technique result shows the ML overall accuracy and kappa coefficient higher than the SVM technique. The main reasons are to increase overall accuracy and kappa coefficient in ML use Sieve Classes, Clump Classes and Majority/Minority Analysis for land cover mapping. These three steps with removes isolated classified pixels, the class information would be contaminated by adjacent class codes and change spurious pixels within a large single class to that class, respectively, improves the amount of outputs. Also, the amount of climbing these values can be with possibly due to the higher image quality and on-time training sample sites to be connected.

References

[1]   Y. Ban, A. Jacob, P. Gamba, "Spaceborne SAR data for global urban mapping at 30m resolution using a robust urban extractor," *ISPRS J. Photogramm. Remote Sens*. vol. 103, no. January 2018, pp. 28–37, 2014.

[2]   F. Cumo, D. A.Garcia, V. S.Pennucci, M. Tiberi, "Technologies and strategies to design sustainable tourist accommodations in areas of high environmental value not connected to the electricity grid", *Int. J. of Sustainable Development and Planning*. vol. 10, no. 1, pp. 20-28, 2015.

[3]   D. Astiaso Garcia, G. Canavero, F. Ardenghi, M. Zambon, "Analysis of wind farm effects on the surrounding environment: Assessing population trends of breeding passerines," *Renewable Energy*. vol. 80, pp. 190-196, 2015.

[4]   U. D. Matteo, P. M. Pezzimenti, D. A. Garcia, "Methodological proposal for optimal location of emergency operation centers through multi-criteria approach", *Sustainability (Switzerland),* vol. 8, no. 1, pp. 1-12, 2016.

[5]   G.Harik, I. Alameddine, R. Maroun, G.Rachid, D. Bruschi, D. A. Garcia, M. El-Fadel, "Implications of adopting a biodiversity-based vulnerability index versus a shoreline environmental sensitivity index on management and policy planning along coastal areas," *Journal of environmental management*, vol. 187, pp. 187-200, 2017.

[6]   D. A. Garcia, D. Bruschi, F. Cumo, F. Gugliermetti,"The Oil Spill Hazard Index (OSHI) elaboration. An oil spill hazard assessment concerning Italian hydrocarbons maritime traffic," *Ocean and Coastal Management*, vol. 80, pp. 1-11, 2013.

[7]   D. A. Garcia, "Green areas management and bioengineering techniques for improving urban ecological sustainability," *Sustainable Cities and Society*, vol. 30, pp. 108-117, 2017.

[8]   D. Groppi, L. de Santoli, F. Cumo, D. A. Garcia, "A GIS-based model to assess buildings energy consumption and usable solar energy potential in urban areas," *Sustainable Cities and Society*, vol. 40, pp. 546-558, 2018.

[9]   D. A. Garcia, F. Cumo, F. Giustini, E. Pennacchia, A. M. Fogheri, "Eco-architecture and sustainable mobility: An integrated approach in Ladispoli town," *WIT Transactions on the Built Environment*, pp. 59, 2014.

[10] D. A. Garcia, F. Cumo, E. Pennacchia. V. Sforzini, "A sustainable requalification of bracciano lake waterfront in trevignano Romano," *International Journal of Sustainable Development and Planning*, vol. 10, no. 2, pp. 155-164, 2015.

[11] D. Bruschi, D. A. Garcia, F. Gugliermetti, F. Cumo, "Characterizing the fragmentation level of Italian's National Parks due to transportation infrastructures," *Transportation Research Part D: Transport and Environment*, vol. 36, pp. 18-28, 2015.

[12] S. Raghuvanshi, D.A. Garcia, R. Hong, L Bellia, B. I. Palella, G. Riccio, G. Cuccurullo, E. Chatzilari, L. Stabile, J. Mačiukaitienė, G. Ficco, A. Russi, G. Giovinco, A. Frattolillo, "A General Approach for Retrofit of Existing Buildings Towards NZEB: The Windows Retrofit Effects on Indoor Air Quality and the Use of Low Temperature District Heating,"IEEE International Conference on Environment and Electrical Engineering and 2018 IEEE Industrial and Commercial Power Systems Europe (EEEIC / I&CPS Europe), 2018. 1-6.

[13] D. Groppi, D. A. Garcia, G. L. Basso, F. Cumo, L. D. Santoli, "Analysing economic and environmental sustainability related to the use of battery and hydrogen energy storages for increasing the energy independence of small islands," Energy Conversion and Management, 177, 64-76, 2018.

[14] D. Groppi, D. A. Garcia, G. L. Basso, L. D. Santoli, "Synergy between smart energy systems simulation tools for greening small mediterranean islands," Renewable Energy, 135, 515-524, 2019.

[15] G. Guidi et al, "Influence of environmental, economic and social factors on a site selection index methodology for a technological centre for radioactive waste management," Chemical Engineering Transactions, vol. 18, 505-510, 2009.

[16] D. A. Garcia, F. Cumo, E. Pennacchia, V. S. Pennucci, G. Piras, V. D. Notti, R. Roversi, "Assessment of a urban sustainability and life quality index for elderly," *International Journal of Sustainable Development and Planning*, vol. 12, no. 5, pp. 908-921, 2017.

[17] L. De Santoli, D. A. Garcia, A. C. Violante, "Planning of flood defence management and rehabilitation of the natural habitat in the downstream part of the river Tiber," *WIT Transactions on the Built Environment*, pp. 25, 2008.

[18] D. Astiaso Garcia, D. Bruschi, F. Cinquepalmi, F. Cumo, "An estimation of urban fragmentation of natural habitats: Case studies of the 24 italian national parks," *Chemical Engineering Transactions*, vol. 32, pp. 49-54, 2013.

[19] D. Astiaso Garcia, S. Sangiorgio, F. Rosa, "Estimating the potential biomasses energy source of forest and agricultural residues in the Cinque Terre Italian National Park," *Energy Procedia*, pp. 674, 2015.

[20] N. Arslan. Assessment of oil spills using Sentinel 1 C-band SAR and Landsat 8 multispectral sensors," Environ Monit Assess. vol. 190, no. 11, pp. 1–14, 2018.

[21] F. Cumo, F. Cinquepalmi, D. Astiaso Garcia, "Data gathering guidelines for the mapping of environmental sensitivity to oil spill of the Italian coastlines," *WIT Transactions on the Built Environment*, pp. 119, 2008.

[22] L. D. Santoli, F. Cumo, D. A. Garcia, D. Bruschi,"Coastal and marine impact assessment for the development of an oil spill contingency plan: The case study of the east coast of Sicily," *WIT Transactions on Ecology and the Environment*, vol. 149, pp. 285-296, 2011.

[23] D. Astiaso Garcia, F. Cinquepalmi, F. Cumo, "Air quality in Italian small harbours: A proposed assessment methodology," *Rendiconti Lincei*, vol. 24, no. 4, pp. 309-318, 2013.

[24] L. Gugliermetti, D. Astiaso Garcia, "A cheap and third-age-friendly home device for monitoring indoor air quality," *International Journal of Environmental Science and Technology*, vol. 15, no. 1, pp. 185-198, 2018.

[25] D. Astiaso Garcia, F. Cumo, F. Gugliermetti, F. Rosa, "Hazardous and noxious substances (HNS) risk assessment along the Italian coastline," *Chemical Engineering Transactions*, vol. 32, pp. 115-120, 2013.

[26] A. Lefebvre, C. Sannier, and T. Corpetti, "Monitoring urban areas with Sentinel-2A data: Application to the update of the Copernicus High Resolution Layer Imperviousness Degree," *Remote Sens.,* vol. 8, no. 7, pp. 1–21, 2016.

[27] D. Astiaso Garcia, D. Bruschi, "A risk assessment tool for improving safety standards and emergency management in Italian onshore wind farms," *Sustainable Energy Technologies and Assessments*, vol. 18, pp. 48-58, 2016.

[28] H. Zakeri, F. Yamazaki, W. Liu, "Texture Analysis and Land Cover Classification of Tehran Using Polarimetric Synthetic Aperture Radar Imagery," *Appl. Sci.*, vol. 7, no. 5, p. 452, 2017.

[29] R. Goldblatt, M. F. Stuhlmacher, B. Tellman, N. Clinton, G. Hanson, M. Georgescu, C. Wang, F. S.Candelad, A. K. Khandelwal, W. H. Cheng, C. Robert, J. R. Balling, "Using Landsat and nighttime lights for supervised pixel-based image classification of urban land cover," *Remote Sens. Environ.*, vol. 205, no. December 2017, pp. 253–275, 2018.

[30] C. Pelletier, S. Valero, J. Inglada, N. Champion, G. Dedieu, "Assessing the robustness of Random Forests to map land cover with high resolution satellite image time series over large areas," *Remote Sens. Environ.*, vol. 187, pp. 156–168, 2016.

[31] H. Zhang, J. Li, T. Wang, H. Lin, Z. Zhenge, Y. Li, Y. Lu, "A manifold learning approach to urban land cover classification with optical and radar data," *Landsc. Urban Plan*, vol. 172, no. December 2017, pp. 11–24, 2018.

[32] N. Tatar, M. Saadatseresht, H. Arefi, A. Hadavand, "A robust object-based shadow detection method for cloud-free high resolution satellite images over urban areas and water bodies," *Adv. Sp. Res.*, vol. 61, no. 11, pp. 2787–2800, 2018.

[33] H. Zhang, R. Xu, "Exploring the optimal integration levels between SAR and optical data for better urban land cover mapping in the Pearl River Delta," *Int. J. Appl. Earth Obs. Geoinf.,* vol. 64, pp. 87–95, 2018.

[34] U. P. Kreuter, H. G. Harris, M. D. Matlock, and R. E. Lacey, "Change in ecosystem service values in the San Antonio area, Texas," *Ecol. Econ.*, vol. 39, no. 3, pp. 333–346, 2001.

[35] S. Aronoff, "Classification Accuracy : A User Approach," [Online]. Available: https://www.asprs.org/wp-content/uploads/pers/1982journal/aug/1982_aug_1299-1307.pdf

[36] M. A. Kalkhanl, R. M. Reich, R. L. Czaplewski, "Statistical Properties of Measures of Association and the Kappa Statistic for Assessing the Accuracy of Remotely Sensed Data Using Double Sampling." [Online]. Available: https://www.fs.fed.us/rm/pubs_rm/rm_gtr277/rm_gtr277_467_476.pdf

[37] S. Koukoulas, G. A. Blackburn, "Introducing New Indices for Accuracy Evaluation of Classified Images Representing Semi-Natural Woodland Environments." *Photogramm. Eng. Remote Sens.*, vol. 67, no. 4, pp. 499–510, 2001.

[38] G. H. Rosenfield, and K. F. Lins, "A Coefficient of Agreement as a Measure of Thematic Classification Accuracy," [Online]. Available: https://www.asprs.org/wp-content/uploads/pers/1986journal/feb/1986_feb_223-227.pdf

[39] G. M. Foody, "Status of land cover classification accuracy assessment," *Remote Sens. Environ.,* vol. 80, no. 1, pp. 185–201, 2002.

[40] A. Lefebvre, C. Sannier, T. Corpetti, "Monitoring urban areas with Sentinel-2A data: Application to the update of the Copernicus High Resolution Layer Imperviousness Degree," *Remote Sens.,* vol. 8, no. 7, pp. 1–21, 2016.

[41] H. Zakeri, F. Yamazaki, W. Liu, "Texture Analysis and Land Cover Classification of Tehran Using Polarimetric Synthetic Aperture Radar Imagery," *Appl. Sci.,* vol. 7, no. 5, p. 452, 2017.

[42] S. Di Zio, A. Montanari, B. Staniscia, "Simulation of urban development in the City of Rome: Framework, methodology, and problem solving," *J. Transp. Land Use*, vol. 3, no. 2, pp. 85–105, 2010.

[43] L. Sallustio, V. Quatrini, D. Geneletti, P. Corona, M. Marchetti, "Assessing land take by urban development and its impact on carbon storage: Findings from two case studies in Italy," *Environ. Impact Assess. Rev.*, vol. 54, pp. 80–90, 2015.

[44] G. Mountrakis, J. Im, C. Ogole, "Support vector machines in remote sensing: A review," *ISPRS J. Photogramm. Remote Sens.*, vol. 66, no. 3, pp. 247–259, 2011.

[45] J. P. Gálveza, J. F. Mas, G. Moré, J. Cristóbal, M. O. Martínez, A. C. Luz, M. Guèze, M. J. Macía, V. R. García, "Enhanced land use/cover classification of heterogeneous tropical landscapes using support vector machines and textural homogeneity," *Int. J. Appl. Earth Obs. Geoinf.*, vol. 23, no. 1, pp. 372–383, 2013.

[46] C. Huang, L. S. Davis, J. R. G. Townshend, "An assessment of support vector machines for land cover classification," *Int. J. Remote Sens.*, vol. 23, no. 4, pp. 725–749, 2002.

[47] M. Wieland, W. Liu, F. Yamazaki, "Learning change from Synthetic Aperture Radar images: Performance evaluation of a Support Vector Machine to detect earthquake and tsunami-induced changes," *Remote Sens.*, vol. 8, no. 10, 2016.

[48] T. Yuan, H. Lee, H. C. Jung, A. Aierken, E. Beighley, D. E. Alsdorf, R. M. Tshimanga, D. Kim, "Absolute water storages in the Congo River floodplains from integration of InSAR and satellite radar altimetry," *Remote Sens. Environ.*, vol. 201, no. March, pp. 57–72, 2017.